

SPECTROSCOPIC EVIDENCE FOR A SUPERMASSIVE BLACK HOLE IN NGC 4486B

JOHN KORMENDY,^{1, 2, 3} RALF BENDER,² JOHN MAGORRIAN,⁴ SCOTT TREMAINE,^{4, 5} KARL GEBHARDT,⁶
DOUGLAS RICHSTONE,⁶ ALAN DRESSLER,⁷ S. M. FABER,⁸ CARL GRILLMAIR,⁹ AND TOD R. LAUER¹⁰,

Received 1996 December 17; accepted 1997 March 27

ABSTRACT

The stellar kinematics of the low-luminosity elliptical galaxy NGC 4486B have been measured in seeing $\sigma_* = 0''.22$ with the Canada-France-Hawaii Telescope (CFHT) and Subarcsecond Imaging Spectrograph. Lauer and collaborators have shown that NGC 4486B is similar to M31 in having a double nucleus. Here we show that it also resembles M31 in its kinematics. Like M31, NGC 4486B rotates fairly rapidly near the center ($V = 76 \pm 7 \text{ km s}^{-1}$ at $0''.6$) but more slowly farther out ($V \simeq 20 \pm 6 \text{ km s}^{-1}$ at $r \simeq 4''$). Also, the velocity dispersion gradient is very steep: σ increases from $116 \pm 6 \text{ km s}^{-1}$ at $r = 2'' - 6''$ to $\sigma = 281 \pm 11 \text{ km s}^{-1}$ at the center. This is much higher than expected for an elliptical galaxy of absolute magnitude $M_B \simeq -16.8$: even more than M31, NGC 4486B is far above the scatter in the Faber-Jackson correlation between σ and bulge luminosity. Therefore the King core mass-to-light ratio, $M/L_V \simeq 20$, is unusually high compared with normal values for old stellar populations ($M/L_V = 4 \pm 1$ at $M_B \simeq -17$).

We construct simple dynamical models with isotropic velocity dispersions and show that they reproduce black hole (BH) masses derived by more detailed methods. We also fit axisymmetric, three-integral models. Isotropic models imply that NGC 4486B contains a central dark object, probably a BH, of mass $M_\bullet = 6_{-2}^{+3} \times 10^8 M_\odot$. However, anisotropic models fit the data without a BH if the ratio of radial to azimuthal dispersions is ~ 2 at $r \simeq 1''$. Therefore this is a less strong BH detection than the ones in M31, M32, and NGC 3115. A dark mass of $6 \times 10^8 M_\odot$ is $\sim 9\%$ of the mass M_{bulge} in stars; even if M_\bullet is somewhat smaller than the isotropic value, $M_\bullet/M_{\text{bulge}}$ is likely to be unusually large.

Double nuclei are a puzzle because the dynamical friction timescales for self-gravitating star clusters in close orbit around each other are short. Since both M31 and NGC 4486B contain central dark objects, our results support models in which the survival of a double nucleus is connected with the presence of a BH. For example, they support the Keplerian eccentric disk model due to Tremaine.

Subject headings: black hole physics – galaxies: individual (NGC 4486B) – galaxies: kinematics and dynamics – galaxies: nuclei

1. INTRODUCTION

NGC 4486B is a low-luminosity E1 companion of M87. From the ground, it looks like a normal dwarf elliptical similar to but slightly brighter than M32. Faber (1973) suggests that it has been tidally truncated by M87; it may once have been brighter than its present absolute magnitude, $M_B \simeq -16.8$ (assumed distance = 16 Mpc).

NGC 4486B was added to the CFHT BH survey (see Kormendy 1993; Kormendy & Richstone 1995, hereafter KR95, for reviews) because *Hubble Space Telescope* (HST) WFPC1 images showed an elongated, asymmetrical center (Lauer *et al.* 1995). If the double nucleus of M31 (Lauer *et al.* 1993) were moved several times farther away, it would look similarly asymmetric. Close double nuclei are a surprise because their orbital decay timescales are short. At least one promising explanation requires a central BH (Tremaine 1995; see § 5, below). This makes NGC 4486B an interesting target for the BH search.

HST WFPC2 images now prove that NGC 4486B has a double center (Lauer *et al.* 1996). Therefore the result of the present paper – that it also contains a massive dark object (MDO) of mass $M_\bullet \gtrsim 10^8 M_\odot$ – leaves us with two cases of double nuclei found in the presence of MDOs. This suggests that the two phenomena are related.

2. CFHT SIS SPECTROSCOPY

The observations were obtained with the CFHT and the Subarcsecond Imaging Spectrograph (SIS). The slit was aligned with the two nuclei. Parameters of the reduced spectra are given in Table 1. SIS includes a tip-tilt guider; by offsetting the guide probe, we centered the galaxy on the slit to $1/4$ pixel = $0''.04$. An exposure sequence consisted of spectrograph rotation, telescope focus, exposures without the grism and slit to center the object, an exposure with the slit in place but with no grism, the object spectrum, another image through the slit but without the grism, one with neither slit nor grism, and a comparison spectrum. Between the beginning and the end of a spectral exposure, the average drift of the galaxy position was $0''.08 \pm 0''.01$ along the slit and $0''.015 \pm 0''.020$ perpendicular to it.

The seeing was measured on the bracketing direct images. Brightness profiles of the galaxy along the slit were measured on these and on the spectrum; they agree (Fig. 1), so the PSF was the same for the spectrum and the direct images. Its Gaussian dispersion radius is $\sigma_* = 0''.28 \pm 0''.02$ (FWHM = $0''.66 \pm 0''.05$) for the average of four, 1800 s exposures and $\sigma_* = 0''.22$ for the best exposure.

After CCD preprocessing and cosmic-ray cleaning, the Ca II infrared triplet region of each spectrum was rewritten on a $\log \lambda$ scale. NGC 4486B is small, so sky spectra from the outer parts of the object spectra were subtracted.

¹ Visiting Astronomer, Canada–France–Hawaii Telescope, operated by the National Research Council of Canada, the Centre National de la Recherche Scientifique of France, and the University of Hawaii.

² Universitäts-Sternwarte, Scheinerstraße 1, München 81679, Germany.

³ Institute for Astronomy, University of Hawaii, 2680 Woodlawn Dr., Honolulu, HI 96822.

⁴ Canadian Institute for Theoretical Astrophysics, University of Toronto, 60 St. George Street, Toronto M5S 3H8, Canada.

⁵ Cosmology Program, Canadian Institute for Advanced Research.

⁶ Dept. of Astronomy, University of Michigan, Ann Arbor, MI 48109.

⁷ Carnegie Observatories, 813 Santa Barbara St., Pasadena, CA 91101.

⁸ UCO/Lick Observatory, Univ. of California, Santa Cruz, CA 95064.

⁹ Jet Propulsion Laboratory, Mail Stop 183-900, 4800 Oak Grove Drive, Pasadena, CA 91109.

¹⁰ Kitt Peak National Observatory, National Optical Astronomy Observatories, P. O. Box 26732, Tucson, AZ 85726.

TABLE 1
PARAMETERS OF SPECTRA

Parameter	Value
Dates of observations	1996 April 25 – 27
Slit position angle	87°
Slit length	168''
Scale along slit	0''15 pixel ⁻¹
Slit width	0''37
Wavelength range (1024 pixels)...	7580–9405 Å
Reciprocal dispersion	1.781 Å pixel ⁻¹
Reciprocal dispersion	63.3 km s ⁻¹ pixel ⁻¹
Comparison line FWHM	2.19 pixel
Instrumental velocity dispersion	59 km s ⁻¹
Standard star	η Cyg (K0 III)

3. KINEMATIC RESULTS

Velocities and velocity dispersions were calculated with Bender’s (1990) Fourier correlation quotient program. Results are given in Table 2 and Fig. 1. The middle section of Table 2 is for the $\sigma_* = 0''.22$ spectrum; the top and bottom sections are for the average of all four spectra.

Since both galaxies have double nuclei, it is interesting to compare NGC 4486B with M31. However, note that M31 is better resolved by the available spectroscopy than is NGC 4486B. In M31, the separation of the nuclei is 1.8 pc = 0''.49 (Lauer *et al.* 1993), comparable to the best spectroscopic resolution (FWHM = 0''.64, Kormendy & Bender 1996; see KR95) and much larger than the spectroscopic scale (0''.0864 pixel⁻¹). In contrast, the nuclei of NGC 4486B are separated by 12 pc = 0''.15 (Lauer *et al.* 1996), i. e. one spectroscopic pixel and much less than the spectroscopic seeing, FWHM = 0''.52 (see Fig. 1).

NGC 4486B is kinematically similar to M31. Both galaxies have rotation curves that increase toward the center to apparent maximum velocities that are limited by seeing. In M31, $V_{\max} = 157 \pm 4$ km s⁻¹ and in NGC 4486B, $V_{\max} = 76 \pm 7$ km s⁻¹. Outside the spinning center, V is only 10–20 km s⁻¹ at $r \simeq 4''$ in both galaxies. (At still larger radii, bulge rotation is important in M31.) Similarly, the velocity dispersion at large radii is normal for the luminosity of the bulge (see Fig. 2) but then increases rapidly to remarkably large values at the center. Like V_{\max} , the apparent maximum velocity dispersion is limited by seeing; it is 246 ± 8 km s⁻¹ at $\sigma_* = 0''.27$ in M31 and 281 ± 11 km s⁻¹ at $\sigma_* = 0''.22$ in NGC 4486B.

There are also signs of kinematic asymmetries like those in M31. The velocity dispersion is higher on the W side of the center (“P2” in Lauer *et al.* 1996) than on the E side. The velocity zero radius is displaced by $0''.11 \pm 0''.03$ from P2 toward P1. And the P1 side rotates somewhat more rapidly. These effects are marginal at the present resolution and should be checked with *HST* spectroscopy.

The central σ is much larger than we would expect from the Faber-Jackson (1976) correlation between σ and M_B (Fig. 2). The best stellar-dynamical BH candidates, M31 (Dressler & Richstone 1988; Kormendy 1988) and NGC 3115 (Kormendy & Richstone 1992; Kormendy *et al.* 1996) stand out: their central velocity dispersions are above the scatter for other objects. NGC 4486B is similarly above the scatter: $\sigma = 281 \pm 11$ km s⁻¹ is surprisingly high for such a low-luminosity galaxy. Even if NGC 4486B has been tidally stripped, σ would have been above the scatter

TABLE 2
NGC 4486B MAJOR-AXIS KINEMATICS

r	V	$\epsilon(V)$	σ	$\epsilon(\sigma)$
–4.52	34	19	112	24
–2.96	18	14	140	15
–2.21	40	7	119	8
–1.70	46	11	164	11
–1.30	66	10	168	11
–1.09	83	14	179	17
–0.94	73	9	172	11
–0.79	75	15	204	20
–1.11	89	16	181	15
–0.75	62	20	233	24
–0.51	56	13	228	15
–0.30	61	22	281	25
–0.15	52	23	267	24
0.00	44	21	291	25
0.15	–47	18	284	19
0.30	–82	13	180	15
0.53	–93	16	194	18
0.75	–100	17	218	15
1.11	–63	14	156	17
0.86	–86	12	172	14
1.01	–70	15	174	16
1.23	–64	11	168	11
1.60	–57	9	144	11
2.57	–40	10	113	12
3.70	–10	11	110	10
5.51	–26	21	98	35

of other objects for any plausible progenitor luminosity. Of course, the BH galaxies in Fig. 2 have been measured with better resolution than most other galaxies. Our comments are not meant to imply that these others do not contain BHs; they may move upward too when they are observed at high resolution. But the scatter of points in Fig. 2 shows the range of σ values for which the central mass-to-light ratio is normal for an old stellar population. With respect to these, BH candidates stand out as having large σ .

For a resolved core, the King core mass-to-light ratio (Richstone & Tremaine 1986) provides a good indication of whether there is extra dark matter near the center. Where Σ_0 is the central surface brightness, r_c is the core radius, and G is the gravitational constant,

$$\frac{M}{L} = \frac{9\sigma^2}{2\pi G \Sigma_0 r_c}. \quad (1)$$

Kormendy (1993) emphasizes that $\Sigma_0 r_c \simeq$ constant in different galaxies, so it is usually not r_c or Σ_0 that determines whether an object has a high M/L ratio. Instead, M/L is high or low if σ^2 is high or low compared to other galaxies. For $\sigma = 281$ km s⁻¹, $r_c \simeq 0''.23$, and Σ_0 corresponding to 14.26 V mag arcsec⁻², the core mass-to-light ratio is $M/L_V \simeq 20$. This is much higher than values (4 ± 1 at $M_B \simeq -16.8$) normally observed in old stellar populations. Therefore NGC 4486B’s high velocity dispersion suggests that it contains an MDO.

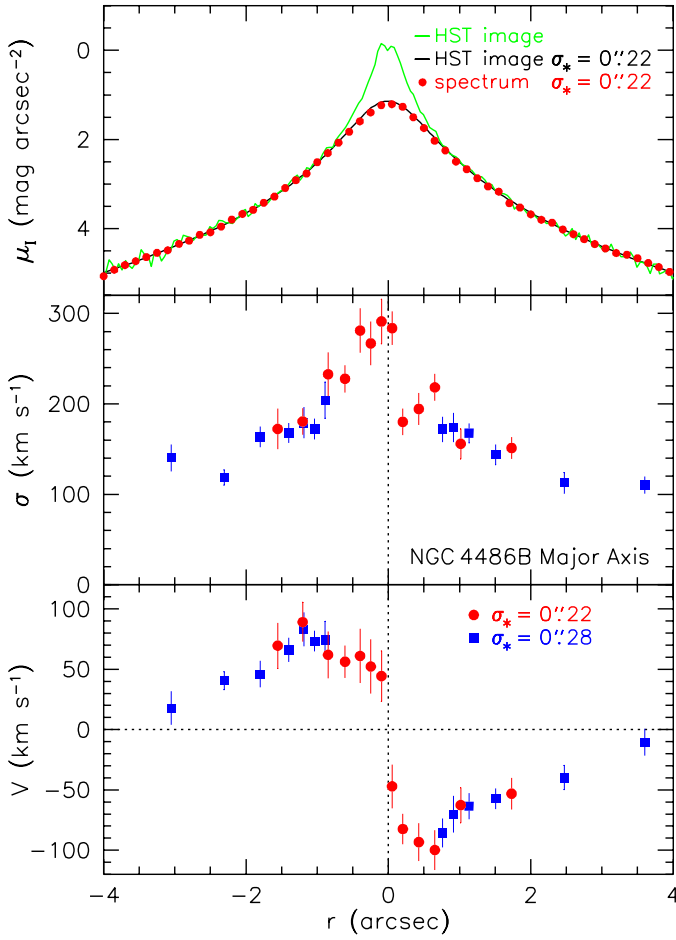


FIG. 1.—Surface brightnesses and kinematics along the major axis of NGC 4486B. In the top panel, the lower solid line is for the deconvolved *HST* image (Lauer *et al.* 1996) convolved with our PSF. Filled circles show the brightness profile measured from our best spectrum.

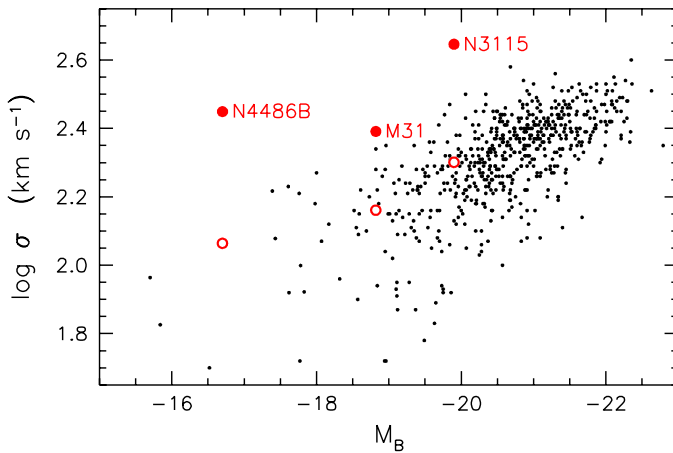


FIG. 2.—Correlation of $\log \sigma$ with M_B for 594, E and S0 galaxies from McElroy (1995) and for faint ellipticals from Bender, Burstein, & Faber (1992). Distances are based on a Hubble constant of $H_0 = 75 \text{ km s}^{-1} \text{ Mpc}^{-1}$ as in McElroy (1995). Filled circles show apparent central velocity dispersions for M31 (CFHT: $\sigma_* = 0''.27$), NGC 3115 (*HST*, aperture = $0''.21$), and NGC 4486B (present data). Open symbols are bulge dispersions outside the region affected by the MDO.

4. SPHERICAL ISOTROPIC DYNAMICAL MODELS

Detailed mass modeling of NGC 4486B is postponed until *HST* spectroscopy becomes available. Here we take a first look at whether NGC 4486B contains an MDO by constructing spherical, isotropic dynamical models. The gravitational potential due to the stars is calculated from the brightness distribution, a central MDO is added, and the parameters of both are varied until a match is obtained to $(V^2 + \sigma^2)^{1/2}$. Output are the allowed range of stellar mass-to-light ratios M/L_V and MDO masses M_\bullet .

The models are constructed as follows. First, we find the galaxy's intrinsic light distribution $\nu(r)$ by deprojecting its surface brightness profile. We assume that M/L_V is independent of radius except for M_\bullet , and we derive the model potential $\Phi(r)$ by solving the Poisson equation. For each assumed M_\bullet , we then integrate the Jeans equation,

$$\frac{d}{dr} (\nu \sigma^2) = -\nu \frac{d\Phi}{dr} \quad (2)$$

to find the intrinsic second-order moment $\nu \sigma^2(r)$. We project this and the zeroth-order moment $\nu(r)$ along each line of sight and convolve the results with the spectroscopic seeing. Finally, we average the seeing-convolved zeroth- and second-order moments over the bins used in the spectroscopy. Dividing each second-order moment by the corresponding zeroth-order moment and taking the square root yields the predicted dispersion profile to be compared with the data. Error estimates on M_\bullet include only the uncertainty in the σ data; they do not take into account differences between velocity measurements and velocity moments, errors in the assumptions (e. g., anisotropy effects), or distance errors.

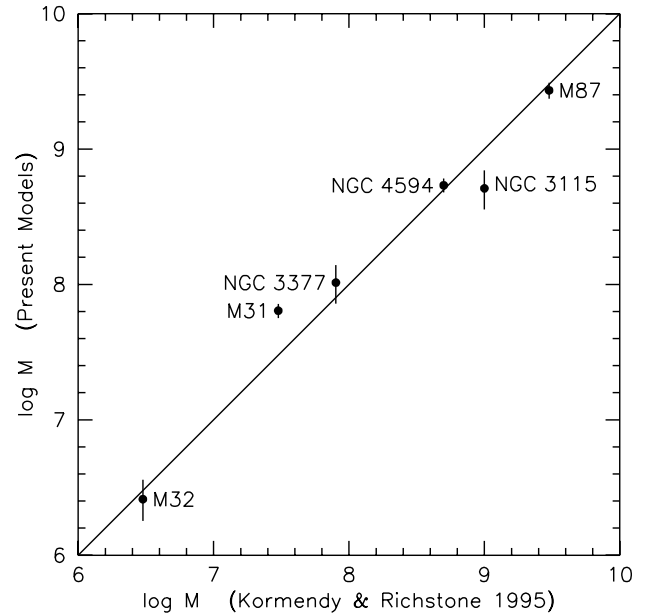


FIG. 3.—Comparison of BH masses obtained using the present, simple modeling technique with masses (KR95) derived via more detailed models (e. g., including rotation).

Figure 3 compares BH masses derived as above with those obtained from more detailed models (see KR95 for references). The highest-resolution ground-based results are used; these match the resolution of the present data. Only M32 has been updated since KR95 (Bender *et al.* 1996). Figure 3 shows that for most objects the present technique reproduces the published BH masses to better than a factor of two.

5. A SUPERMASSIVE BH IN NGC 4486B

The machinery of §4 was used to fit the *HST* WFPC2 photometry in Lauer *et al.* (1996) and the kinematic data in Fig. 1. The results are shown in Fig. 4. These models imply that NGC 4486B contains an MDO with $M_{\bullet} \simeq 8.7 \times 10^8 M_{\odot}$. The corresponding stellar mass-to-light ratio is $M/L_V = 5.0$. As in other MDO detections, the most probable interpretation is a supermassive BH.

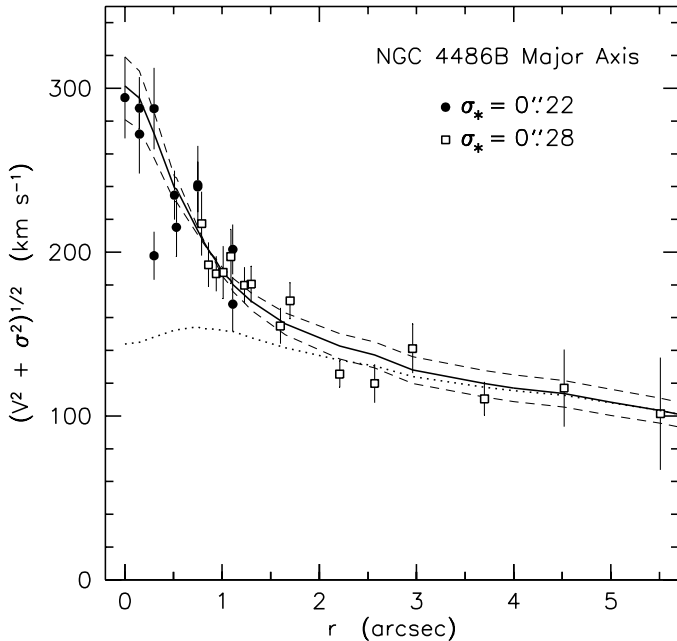


FIG. 4.—Fits of spherical, isotropic models to the kinematics of NGC 4486B. The solid line is the best-fitting model ($M_{\bullet} = 8.7 \times 10^8 M_{\odot}$; $M/L_V = 5.0$). The dashed lines are “error bar” models with $M_{\bullet} = 10.5 \times 10^8 M_{\odot}$; $M/L_V = 3.8$ and $M_{\bullet} = 6.9 \times 10^8 M_{\odot}$; $M/L_V = 6.3$. The dotted line fitted at large radii is a no-BH model with $M/L_V = 6.4$.

However, this is a weaker BH detection than the best stellar-dynamical cases (the Galaxy, M 31, M 32, and NGC 3115). The reason is that axisymmetric, three-integral maximum entropy models (Richstone *et al.* 1996) can fit the data without a BH provided that the ratio of radial to azimuthal velocity dispersions is $\sigma_r/\sigma_{\theta} \simeq \sigma_r/\sigma_{\phi} \simeq 2$ at $r \simeq 1''$. Since rotation is relatively unimportant in NGC 4486B, some anisotropy would not be surprising. On the other hand, anisotropic models may be unstable (Merritt 1987). Also, isotropic model measurements of M_{\bullet} have turned out to be close to correct when anisotropic models were constructed (see KR95 for a review). E. g., in M 87, the Sargent *et al.* (1978) measurement of M_{\bullet} has turned out to be remarkably accurate (Harms *et al.* 1994) even though the galaxy is so luminous that anisotropy is almost assured and even though anisotropies can explain the kinematics without a BH (Duncan & Wheeler 1980; Binney & Mamon 1982; Richstone & Tremaine 1985; Dressler & Richstone 1990; van der Marel 1994). Therefore it is likely that M_{\bullet} in NGC 4486B is close to but somewhat smaller than the value given above. Even nearly isotropic maximum entropy models give a smaller mass than those of Fig. 4, i. e., $M_{\bullet} \simeq 4 \times 10^8 M_{\odot}$. In this case, the stellar mass-to-light ratio $M/L_V \simeq 7$ is unusually high for a galaxy of $M_B = -16.8$, while the models of Fig. 4 imply a more nearly normal mass-to-light ratio. Therefore:

We adopt the mean of the Jeans and maximum entropy model results, $M_{\bullet} = 6_{-2}^{+3} \times 10^8 M_{\odot}$ and $M/L_V = 6 \pm 1$.

This is a remarkably large BH mass for such a low-luminosity galaxy. It is well above the correlation between M_{\bullet} and bulge luminosity that is observed for other galaxies (Fig. 5). For ten previous BH detections, the mean ratio of M_{\bullet} to the mass of the bulge is $\langle M_{\bullet}/M_{\text{bulge}} \rangle = 0.0022_{-0.0009}^{+0.0014}$. To date, NGC 3115 has had the largest BH mass fraction, 2.4%. But $6 \times 10^8 M_{\odot}$ is $9.4_{-3.5}^{+5.0}$ % of the mass in stars. Even if the galaxy once was brighter, its BH mass is surprisingly high. In fact, NGC 4486B is a good model of what a nearly naked quasar (Bahcall *et al.* 1994, 1995, 1996) would look like after it turned off: a monstrous BH in a tiny galaxy. However, since anisotropic models allow smaller BH masses, it will be important to check this result when *HST* spectroscopy becomes available.

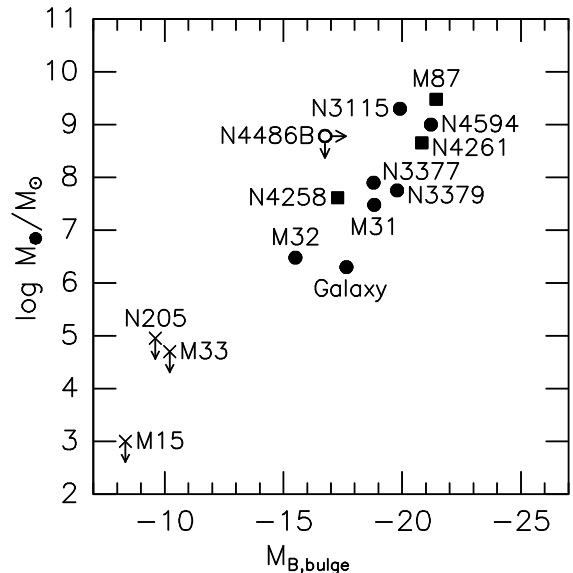


FIG. 5.—BH mass as a function of bulge absolute magnitude, from KR95 but with BH masses updated for M 32, NGC 3115, and NGC 4594, and with NGC 205 (Jones *et al.* 1996), NGC 4261 (Ferrarese *et al.* 1996), NGC 3379 (Gebhardt *et al.* 1996) and NGC 4486B (this paper) added. Circles and squares show objects with stellar- and gas-dynamical evidence for BHs, respectively. Upper limits on M_{\bullet} are plotted as crosses. The correlation may be only the upper envelope of a distribution that extends to smaller M_{\bullet} .

An MDO detection in NGC 4486B is interesting because one promising explanation for double nuclei requires a BH. Double nuclei pose an interesting problem because they cannot reasonably be two star clusters in orbit around each other: the dynamical friction timescale for the decay of their relative orbits would be short. Also, for two close double nuclei to appear in the present sample of galaxies observed with *HST*, there should be many more at larger separations where merger timescales are still long. These are not seen. Tremaine (1995) therefore developed a model of M 31 in which both nuclei are parts of the same eccentric disk of stars. The brighter nucleus (P1), which is also farther from the barycenter, results from the lingering of stars near apocenter, and the fainter nucleus (P2) results from the disk’s increase in density toward the center. A BH near P2 is required to make the potential almost Keplerian. Only then can an eccentric disk be maintained by modest restoring forces such as the disk’s self-gravity.

NGC 4486B now is a second example of a double nucleus. It, too, contains an MDO. This supports Tremaine's model. The details are different here; neither nucleus is at the galaxy center. If the double nuclei are an embedded disk, then the disk may have a different orientation or a central hole (Lauer *et al.* 1996). More generally, our results support models in which the survival of a double nucleus is connected with the presence of a BH.

We thank D. McElroy for providing a digital copy of his σ catalog. JK is grateful to the Alexander von Humboldt-

Stiftung (Germany) for the Research Award that made possible his visit to the Universitäts-Sternwarte, Ludwig-Maximilians-Universität, Munich. He also thanks the Sternwarte for its hospitality. JK's work was supported by NSF grant AST-9219221. RB's work was supported by SFB 375 of the German Science Foundation and by the Max-Planck-Gesellschaft. The Nuker team was supported by HST data analysis funds through grant GO-02600.01-87A and by NSERC. We thank the Fields Institute for Research in Mathematical Sciences at the University of Toronto for their hospitality during part of this work.

REFERENCES

- Bahcall, J. N., Kirhakos, S., & Schneider, D. P. 1994, *ApJ*, 435, L11
 Bahcall, J. N., Kirhakos, S., & Schneider, D. P. 1995, *ApJ*, 450, 486
 Bahcall, J. N., Kirhakos, S., & Schneider, D. P. 1996, *ApJ*, 457, 557
 Bender, R. 1990, *A&A*, 229, 441
 Bender, R., Burstein, D., Faber, S. M. 1992, *ApJ*, 399, 462
 Bender, R., Kormendy, J., & Dehnen, W. 1996, *ApJ*, 464, L123
 Binney, J., & Mamon, G. A. 1982, *MNRAS*, 200, 361
 Dressler, A., & Richstone, D. O. 1988, *ApJ*, 324, 701
 Dressler, A., & Richstone, D. O. 1990, *ApJ*, 348, 120
 Duncan, M. J., & Wheeler, J. C. 1980, *ApJ*, 237, L27
 Faber, S. M. 1973, *ApJ*, 179, 423
 Faber, S. M., & Jackson, R. E. 1976, *ApJ*, 204, 668
 Ferrarese, L., Ford, H. C., & Jaffe, W. 1996, *ApJ*, 470, 444
 Gebhardt, K., Richstone, D., Kormendy, J., Bender, R., Faber, S., Lauer, T., Magorrian, J., & Tremaine, S. 1996, *BAAS*, 28, 1422
 Harms, R. J., *et al.* 1994, *ApJ*, 435, L35
 Jones, D. H., *et al.* 1996, *ApJ*, 466, 742
 Kormendy, J. 1988, *ApJ*, 325, 128
 Kormendy, J. 1993, in *The Nearest Active Galaxies*, ed. J. Beckman, L. Colina & H. Netzer (Madrid: Consejo Superior de Investigaciones Cientificas), p. 197
 Kormendy, J., & Bender, R. 1996, in preparation
 Kormendy, J., *et al.* 1996, *ApJ*, 459, L57
 Kormendy, J., & Richstone, D. 1992, *ApJ*, 393, 559
 Kormendy, J., & Richstone, D. 1995, *ARA&A*, 33, 581 (KR95)
 Lauer, T. R., *et al.* 1993, *AJ*, 106, 1436
 Lauer, T. R., *et al.* 1995, *AJ*, 110, 2622
 Lauer, T. R., *et al.* 1996, *ApJ*, 471, L79
 McElroy, D. B. 1995, *ApJS*, 100, 105
 Merritt, D. 1987, *ApJ*, 319, 55
 Richstone, D., *et al.* 1996, in preparation
 Richstone, D. O., & Tremaine, S. 1985, *ApJ*, 296, 370
 Richstone, D. O., & Tremaine, S. 1986, *AJ*, 92, 72
 Sargent, W. L. W., *et al.* 1978, *ApJ*, 221, 731
 Tremaine, S. 1995, *AJ*, 110, 628
 van der Marel, R. P. 1994, *MNRAS*, 270, 271